Exact diagonalization of the $S = 1/2$ Heisenberg antiferromagnet on finite bcc lattices to estimate properties on the infinite lattice

1998 J. Phys. A: Math. Gen. 31 7685

(http://iopscience.iop.org/0305-4470/31/38/006)

J. Phys. A: Math. Gen. **31** (1998) 7685–7698. Printed in the UK PII: S0305-4470(98)94747-3

Exact diagonalization of the $S = 1/2$ Heisenberg antiferromagnet on finite bcc lattices to estimate properties on the infinite lattice

D D Betts†‖, J Schulenburg‡, G E Stewart§, J Richter‡¶ and J S Flynn†

† Department of Physics, Dalhousie University, Halifax NS, Canada B3H 3J5

‡ Institut für Theoretische Physik, Universität Magdeburg, PO Box 4120, D-39016 Magdeburg, Germany

§ Pulp and Paper Centre, University of British Columbia, 2385 East Mall, Vancouver BC, Canada V6T 1Z4

Received 29 May 1998

Abstract. This paper is the third in a sequence of papers developing and applying the finite-lattice method for estimation of the zero-temperature properties of quantum spin models on infinite cubic lattices. Here we generate finite bipartite body-centred cubic (bcc) lattices of $16 \leqslant N \leqslant 32$ vertices. Our geometrically distinct finite lattices are defined by vectors in upper triangular lattice form. We have found that sets of two to six geometrically distinct finite bcc lattices are topologically identical, and that we thus need only one lattice of each set for our method of estimation. We have studied the spin one-half Heisenberg antiferromagnet by diagonalizing its Hamiltonian on each of the finite lattices and hence computing its ground-state properties. By extrapolation of these data we obtain estimates of the $T = 0$ properties on the infinite bcc lattice. Our estimate of the $T = 0$ energy agrees to five parts in 10 thousand with third-order spin-wave and series-expansion method estimates, while our estimate of the staggered magnetization agrees with the spin-wave estimate to within 0.25%.

1. Introduction

The physics of quantum spin systems on lattices has been much studied and remains of great interest. It is a major part of condensed matter physics. In particular at zero temperature questions such as what the energy per vertex is, whether long-range order exists, if so what is its nature, the possibility of quantum phase transitions, the spatial dependence of spin–spin correlations, etc are being studied. Several different methods of calculating the properties of quantum spin systems such as the Heisenberg antiferromagnet, the XY ferromagnet and the t–J model are being developed and used. The usefulness of a method of calculation of properties depends greatly on the dimension, d, of the lattice and the temperature, T.

At $T = 0$ and for $d = 2$ or 3 series expansions starting from the Ising model limit and spin-wave methods have proved to be particularly useful [1]. The quantum Monte Carlo method would be very useful too, but we are unaware of its application to quantum spin models on cubic lattices.

In 1964 Bonner and Fisher [2] introduced what we could now call the method of exact diagonalization on finite lattices in one dimension. Two decades ago Oitmaa and Betts

‖ E-mail address: dbetts@is.dal.ca

¶ E-mail address: johannes.richter@physik.uni-magdeburg.de

0305-4470/98/387685+14$19.50

introduced the finite-lattice method in two dimensions [3, 4]. It became popular after high T_c superconductivity was discovered. For further information recent review articles are recommended [5, 6]. However, it seems that until recently (except for one short exploratory paper [7]) no one extended the method of exact diagonalization on finite lattices to three dimensions.

In 1997 Betts and Stewart published their paper on the estimation of zero-temperature properties of quantum spin systems on the simple cubic lattice via exact diagonalization on finite simple cubic lattices [8]. This method was soon extended to finite face centred cubic (fcc) lattices for the estimation of the $T = 0$ properties of the spin one-half XY ferromagnet on the infinite fcc lattice using finite fcc lattices of $N \leqslant 25$ vertices [9]. The finite-lattice method estimates of the energy and magnetization per vertex of this model agreed to within a fraction of a percent with the estimates by spin-wave, series-expansion and variational methods.

We learned from Lyness *et al* [10] about using a triple of vectors in upper triangular lattice form (utlf) to define finite lattices in three dimensions. Generating finite lattices in this way ensures that each lattice is geometrically distinct. Some of us used the utlf method first to define finite lattices [9]. Since then we have learned that some lattices that are geometrically distinct are topologically identical. Hence, as far as we have investigated, each physical property of each quantum spin model with nearest neighbour interactions has the same numerical value on all topologically identical though geometrically distinct lattices.

In section 3 we describe how to classify finite-lattices topologically. First we define a topological neighbourhood matrix and calculate one for each finite bcc lattice. Any two geometrically distinct finite lattices whose neighbourhood matrices are equivalent are topologically identical lattices. We find such equivalence in two separate ways. Our topological sorting code is very easy to calculate but is useful only for bipartite finite lattices of $N < 32$. The little known Smith normal form matrix can work for large as well as small lattices but is more complicated to calculate.

Section 4 describes the computation of the ground-state eigenvalue and eigenvector of the spin one-half Heisenberg Hamiltonian on the finite bcc lattices. Ground-state spin–spin correlations are computed for each lattice using its eigenvector. Thence the staggered magnetization is calculated. Statistical analyses fit formulae, determined by spin-wave theory [1], in $N^{-1/3}$ to the data in turn for energy, magnetization and correlations and thus provide finite-lattice method estimates for the $T = 0$ properties on the infinite bcc lattice. Since our method includes the precise calculation of the ground-state of the eigenvector, it has the advantage of the ready calculation of any property of the quantum spin model based on its ground-state eigenvector.

Finally we compare our finite results with the recent series expansion, third-order spin-wave [1] and variational [11] estimates. Our estimate of the energy per vertex agrees with the spin-wave and series-expansion estimates very closely. Our estimate of the staggered magnetization agrees to within 0.25% with the estimates from both of the above-mentioned methods. The variational estimate of energy is 1% below the other three estimates, and the variational estimate of staggered magnetization is 3% below the other estimates.

2. Generation of bipartite finite bcc lattices

The unbounded bcc lattice can be defined by any three of the primitive vectors $\boldsymbol{a}_1 = (1, 1, 1)$, $\boldsymbol{a}_2 = (1, 1, -1)$, $\boldsymbol{a}_3 = (1, -1, 1)$ and $\boldsymbol{a}_4 = (-1, 1, 1)$. The unbounded bcc lattice can be

filled by identical parallelepipeds each defined by three edge vectors,

$$\boldsymbol{l}_\alpha = \sum_{\beta=1}^{3} n_{\alpha\beta}\boldsymbol{a}_\beta \tag{2.1}$$

where $n_{\alpha\beta}$ are integers.

A finite bcc lattice can be derived from any one of the parallelepipeds described above by being subjected to periodic boundary conditions. That is, each of the three pairs of opposite faces are identified.

A finite bcc lattice is bipartite if each of the nine coefficients, $n_{\alpha\beta}$, is an even integer. The resulting bipartite finite bcc lattice consists of two identical finite simple cubic lattices. Any of several different parallelepipeds can generate the same finite lattice. Another way of regarding a finite lattice is to consider an unbounded lattice, bcc, fcc or whatever, as being composed of N identical sublattices. Then on each of the N sublattices all vertices are considered to be one vertex.

In figure 1 we provide an example of a bipartite finite bcc lattice. The parallelepiped which by replication fills the unbounded bcc lattice is defined by edge vectors

$$\boldsymbol{L}_1 = (0, -2, 4) \qquad \boldsymbol{L}_2 = (2, 4, 0) \qquad \boldsymbol{L}_3 = (-2, 4, 2). \tag{2.2}$$

The volume of this parallelepiped is 72, which means that it contains $N = 18$ vertices. The vertices on one simple cubic sublattice are represented by black circles and those on the other sublattice by white squares. Of course, each of the eight corner vertices is shared by eight parallelepipeds, and each of the two face-centred 'white vertices', $(-1, 1, 3)$ and $(1, 5, 3)$, is shared between two parallelepipeds.

An $N = 18$ bipartite finite bcc lattice is formed by the application of periodic boundary conditions in all three directions, that is, by identifying each pair of opposite faces of the parallelepiped. The resulting nine distinct vertices on one sublattice are labelled $A, B, C, \ldots I$ and the nine vertices on the other sublattice are labelled $a, b, c, \ldots i$. We have drawn bonds only between vertex $(0, 4, 2)$ and its eight nearest neighbours. (Drawing all the bonds would make figure 1 appear too cluttered.) Note that two of these bonds each have two pieces within the parallelepiped, but because of periodic boundary conditions each of these bonds is continuous in the finite lattice.

Since publishing the first paper on exact diagonalization on finite cubic lattices [8] we learned about describing the generating of finite lattices by parallelepipeds in utlf. An $n \times n$ matrix, B, is in upper triangular lattice form [10] if and only if the integral matrix elements, b_{ij}, satisfy the following criteria:

$$\begin{aligned} &b_{ij} \geqslant 1 \qquad i = 1, 2, \ldots, n \\ &b_{ij} = 0 \qquad 1 \leqslant j < i \leqslant n \\ &b_{ij} \in [0, b_{ij}) \qquad 1 \leqslant i < j \leqslant n. \end{aligned} \tag{2.3}$$

For utlf parallelepipeds on the bcc lattice the first edge vector, $\boldsymbol{l}_1$, is in the positive octant of the lattice space but not in the tz-plane; the second edge vector, $\boldsymbol{l}_2$, lies in the positive quadrant of the yz-plane but not along the z-axis; the third edge vector, $\boldsymbol{l}_3$, lies on the positive z-axis. These three edge vectors form a 3×3 utlf matrix, B. By using only generating, or defining, vectors in utlf form each finite lattice is described only once, so we have no need to search for duplicates. Further discussion on utlf matrices is contained in Stewart *et al* [9] and Lyness *et al* [10].

Here we describe our best criteria for the initial selection of finite bipartite bcc lattices. First, each vertex must have eight distinct nearest neighbours for a model such as the usual Heisenberg antiferromagnet. Thus all finite bipartite bcc lattices must have at least 16

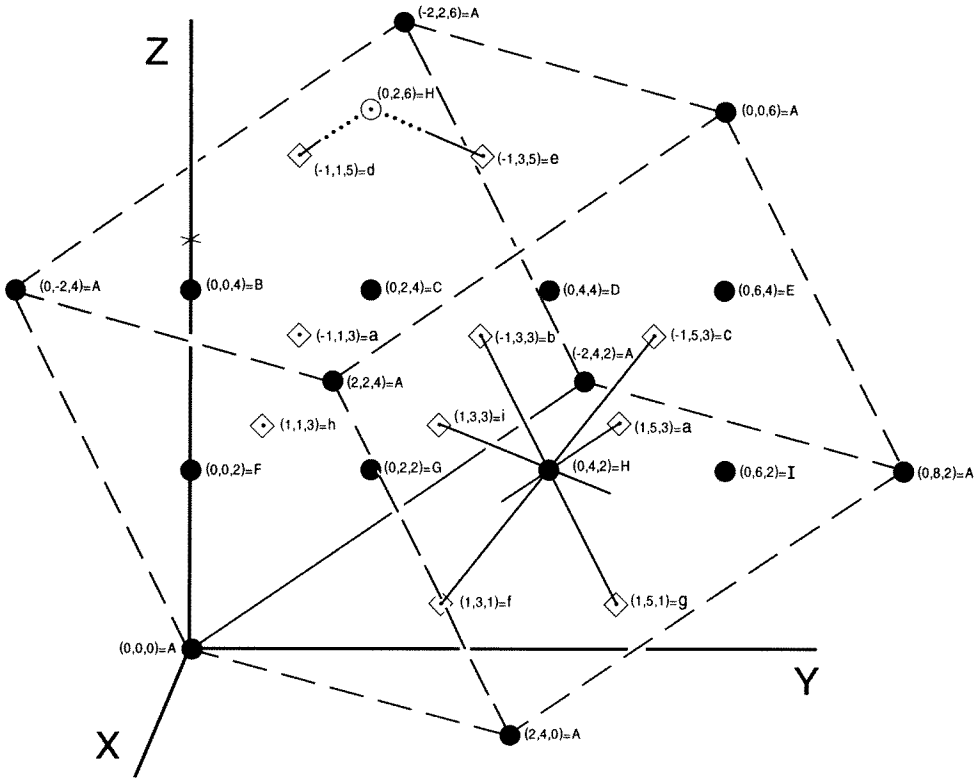

Figure 1. A sample 18 vertex, bcc lattice-filling parallelepiped is defined in this figure by the eight corner vertices and the broken lines between them representing the edges. Application of periodic boundary conditions to this parallelepiped forms the bipartite $N = 18$ bcc lattice. The nine vertices on one sublattice, labelled by capital letters, are represented by full circles, and the vertices on the other sublattice, labelled by lower case letters, are represented by white squares. The full lines connect vertex H to its eight nearest neighbours.

vertices. At the other limit one need not generate bcc lattices of more vertices than the computer can deal with in a reasonable length of time; in our present case $N < 33$. A useful lattice of $N < 31$ should have no pair of vertices farther apart than geometrically seventh neighbours or equivalently topologically third neighbours (as described below). For $31 < N < 41$ lattices topologically fourth neighbours should be included. Such criteria for the bcc and other lattices topologically fourth neighbours should be included. Such criteria for the bcc and other lattices can be applied in a simple computer program. With the computing facilities available to us, we could complete the exact diagonalization of the antiferromagnetic $S = \frac{1}{2}$ Heisenberg Hamiltonian on finite bcc lattices of more than 32 vertices, but it would have taken much more time. However, we are pleased to have computed the ground-state eigenvector of 16 topologically distinct bcc lattices of 32 vertices.

Table 1 gives, for $16 \leqslant N \leqslant 32$, the number of finite bcc lattices that are geometrically distinct, the number of the geometrically distinct lattices that are bipartite, the number of those that are also topologically distinct and finally, the number of those remaining which are also statistically useful in our method.

All topologically distinct bipartite bcc lattices of $16 \leqslant N \leqslant 32$ vertices are described in table 2 below. Each lattice is described by a label $N\alpha$. The 'best' lattice for each N

Table 1. Numbers of finite bcc lattices of even N vertices in which each lattice has eight distinct nearest-neighbour vertices. The number headings are: n_g—geometrically distinct lattices; n_b—bipartite lattices; n_t—topologically distinct bipartite lattices; n_u—statistically useful lattices.

N	n_g	n_b	n_t	n_u
16	12	5	1	1
18	15	1	1	1
20	22	4	2	2
22	16	1	1	1
24	52	15	6	5
26	21	2	2	2
28	44	9	6	4
30	52	7	7	5
32	57	20	16	10
Totals	291	64	42	31

is labelled A, the second best B, etc. The statistical analysis of the energy data for the Heisenberg antiferromagnet described in section 4 determines the order of goodness of the finite lattices. The finite lattices are defined by a set of three vectors, $\boldsymbol{l}_i$, in upper triangular lattice form. One can consider the three vectors as defining the edge of a parallelepiped, and then that the three pairs of opposite faces are identified, thus defining the finite lattice. The same finite lattice can then be defined by a different 'compact' parallelepiped whose compact edge vectors, $\boldsymbol{L}_j$, are as short as possible:

$$\boldsymbol{L}_j = \sum_{i=1}^{3} m_{ji}\boldsymbol{l}_i \tag{2.4}$$

with each coefficient, m_{ji}, being an integer, positive, negative, or zero. The converse linear relation also requires integral coefficients.

3. Topologically distinct finite lattices

After publication of the first article on using finite three-dimensional (simple cubic) lattices to estimate the zero-temperature properties of quantum spin systems [8] we became puzzled over the computed properties of some of the finite lattices. An examination of table 1 in that publication shows that three apparently geometrically distinct $N = 16$ bipartite simple cubic lattices have the same computed ground-state energy and the same long-range order for the Heisenberg antiferromagnet and for the XY ferromagnet. This phenomenon also occurs for a pair of $N = 18$ bipartite simple cubic lattices and a triple of $N = 20$ bipartite simple cubic lattices.

In our second paper [9], developing the finite-lattice method on the fcc lattice for the XY ferromagnet, no such phenomenon was found. However, there are no bipartite fcc lattices. When we turned to the Heisenberg antiferromagnet on the bcc lattice the same phenomenon *was* manifest. We wondered whether such geometrically distinct finite lattices, simple cubic or bcc, could be topologically identical.

Our first step in determining whether two geometrically distinct finite lattices of N vertices are also topologically distinct is to construct a *topological neighbourhood matrix* for each finite lattice. We label the vertices $a, b, c, \ldots$ on one sublattice and $A, B, C, \ldots$ on the other. Suppose an imaginary microscopic frog can hop from one vertex to only one

Table 2. Defining vectors of topologically distinct bipartite bcc lattices of $16 \leqslant N \leqslant 32$ vertices.

	utlf vectors			Compact vectors		
$N\alpha$	$\boldsymbol{l}_1$	$\boldsymbol{l}_2$	$\boldsymbol{l}_3$	$\boldsymbol{L}_1$	$\boldsymbol{L}_2$	$\boldsymbol{L}_3$
16*A*	(4, 0, 0)	(0, 4, 0)	(0, 0, 4)	(4, 0, 0)	(0, 4, 0)	(0, 0, 4)
18*A*	(2, 0, 8)	(0, 2, 4)	(0, 0, 18)	(2, −2, 4)	(0, 2, 4)	(4, 0, −2)
20*A*	(2, 0, 10)	(0, 2, 6)	(0, 0, 20)	(2, −2, 4)	(−2, 4, 2)	(4, 0, 0)
20*B*	(2, 0, 8)	(0, 2, 4)	(0, 0, 20)	(2, −2, 4)	(0, 2, 4)	(4, 0, −4)
22*A*	(2, 0, 8)	(0, 2, 4)	(0, 0, 22)	(2, −2, 4)	(0, 2, 4)	(4, 2, −2)
24*A*	(2, 0, 8)	(0, 2, 4)	(0, 0, 24)	(2, −2, 4)	(0, 2, 4)	(4, 4, 0)
24*B*	(2, 0, 4)	(0, 4, 4)	(0, 0, 12)	(2, 0, 4)	(0, 4, 4)	(4, 4, 0)
24*C*	(2, 0, 10)	(0, 2, 6)	(0, 0, 24)	(2, −2, 4)	(−2, 4, 2)	(4, 2, −2)
24*D*	(2, 0, 4)	(0, 4, 6)	(0, 0, 12)	(2, 0, 4)	(−2, 4, 2)	(2, 4, −2)
24*E*	(2, 0, 12)	(0, 2, 4)	(0, 0, 24)	(2, −4, 4)	(0, 2, 4)	(4, 0, 0)
24*F**	(2, 0, 12)	(0, 2, 6)	(0, 0, 24)	(4, 0, 0)	(2, −4, 0)	(2, 2, −6)
26*A*	(2, 0, 10)	(0, 2, 4)	(0, 0, 26)	(2, −4, 2)	(0, 2, 4)	(4, 2, −2)
26*B*	(2, 0, 8)	(0, 2, 4)	(0, 0, 26)	(2, −2, 4)	(0, 2, 4)	(4, 4, −2)
28*A*	(2, 0, 12)	(0, 2, 8)	(0, 0, 28)	(2, −2, 4)	(−2, 4, 4)	(2, 4, 0)
28*B*	(2, 0, 12)	(0, 2, 4)	(0, 0, 28)	(2, −4, 4)	(0, 2, 4)	(4, 2, 0)
28*C*	(2, 0, 10)	(0, 2, 4)	(0, 0, 28)	(2, −4, 2)	(0, 2, 4)	(4, 4, 0)
28*D*	(2, 0, 10)	(0, 2, 6)	(0, 0, 28)	(2, −2, 4)	(−2, 4, 2)	(4, 2, −2)
28*E**	(2, 0, 8)	(0, 2, 4)	(0, 0, 28)	(−2, 4, 0)	(0, 2, 4)	(4, 4, −4)
28*F**	(2, 0, 14)	(0, 2, 4)	(0, 0, 28)	(4, 0, 0)	(0, 2, 4)	(2, −6, 2)
30*A*	(2, 0, 12)	(0, 2, 4)	(0, 0, 30)	(2, −4, 4)	(0, 2, 4)	(4, 2, −2)
30*B*	(2, 0, 4)	(0, 6, 0)	(0, 0, 10)	(2, 0, 4)	(4, 0, −2)	(0, 6, 0)
30*C*	(2, 0, 12)	(0, 2, 6)	(0, 0, 30)	(2, −4, 0)	(0, 2, 6)	(4, 2, 0)
30*D*	(2, 0, 12)	(0, 2, 8)	(0, 0, 30)	(2, −2, 4)	(−2, 4, 4)	(4, 2, 2)
30*E*	(2, 0, 10)	(0, 2, 4)	(0, 0, 30)	(2, −4, 2)	(0, 2, 4)	(4, 4, −2)
30*F**	(2, 0, 10)	(0, 2, 6)	(0, 0, 30)	(2, −4, 0)	(−2, 4, 2)	(4, 2, −4)
30*G**	(2, 0, 8)	(0, 2, 4)	(0, 0, 30)	(2, −4, 0)	(0, 2, 4)	(6, 2, −2)
32*A*	(2, 0, 14)	(0, 2, 8)	(0, 0, 32)	(2, −2, 6)	(−2, 4, 2)	(2, 4, −2)
32*B*	(2, 2, 6)	(0, 4, 0)	(0, 0, 16)	(2, 2, 6)	(0, 4, 0)	(4, 4, −4)
32*C*	(2, 0, 4)	(0, 4, 8)	(0, 0, 16)	(2, 0, 4)	(−2, 4, 4)	(4, 4, 0)
32*D*	(2, 2, 4)	(0, 8, 0)	(0, 0, 8)	(2, 2, 4)	(2, −6, 4)	(4, 4, 0)
32*E*	(2, 0, 10)	(0, 2, 4)	(0, 0, 32)	(2, −4, 2)	(0, 2, 4)	(4, 4, −4)
32*F*	(2, 0, 6)	(0, 4, 8)	(0, 0, 16)	(−2, 4, 2)	(4, −4, 4)	(2, 4, −2)
32*G*	(2, 0, 12)	(0, 2, 4)	(0, 0, 32)	(2, −4, 4)	(0, 2, 4)	(4, 4, 0)
32*H*	(2, 0, 10)	(0, 2, 6)	(0, 0, 32)	(2, −2, 4)	(−2, 4, 2)	(4, 4, 0)
32*I*	(2, 0, 12)	(0, 2, 8)	(0, 0, 32)	(2, −2, 4)	(−2, 4, 4)	(4, 2, 0)
32*J**	(4, 0, 4)	(0, 4, 4)	(0, 0, 8)	(4, 0, 4)	(0, 4, 4)	(4, 4, 0)
32*K**	(2, 0, 6)	(0, 4, 4)	(0, 0, 16)	(4, 4, 0)	(0, 4, 4)	(2, −4, 2)
32*L**	(2, 4, 4)	(0, 8, 0)	(0, 0, 8)	(0, 4, 4)	(2, 4, −4)	(2, 4, 4)
32*M**	(2, 0, 14)	(0, 2, 4)	(0, 0, 32)	(4, 2, 0)	(0, 2, 4)	(2, −6, 2)
32*N**	(2, 0, 4)	(0, 4, 4)	(0, 0, 16)	(2, 0, 4)	(0, 4, 4)	(4, 4, −4)
32*P**	(2, 0, 8)	(0, 2, 4)	(0, 0, 32)	(2, −2, 4)	(0, 2, 4)	(2, −6, 4)
32*Q**	(2, 0, 16)	(0, 2, 4)	(0, 0, 32)	(4, 0, 0)	(0, 2, 4)	(2, −6, 4)

* These finite lattices were statistically found to be outriders.

Table 3. Lower-left quadrant of the topological neighbourhood matrix of three $N = 20$ bipartite bcc lattices.

	Lattice 20.1										Lattice 20.2										Lattice 20.3									
	$l_1 = (2, 0, 8)$, $l_2 = (0, 2, 4)$, $l_3 = (0, 0, 20)$										$l_1 = (2, 0, 10)$, $l_2 = (0, 2, 4)$, $l_3 = (0, 0, 20)$										$l_1 = (2, 0, 10)$, $l_2 = (0, 2, 6)$, $l_3 = (0, 0, 20)$									
	A	*B*	*C*	*D*	*E*	*F*	*G*	*H*	*I*	*J*	*A*	*B*	*C*	*D*	*E*	*F*	*G*	*H*	*I*	*J*	*A*	*B*	*C*	*D*	*E*	*F*	*G*	*H*	*I*	*J*
a	1	1	1	1	3	3	1	1	1	1	3	1	1	1	1	3	1	1	1	1	1	1	3	1	1	1	1	3	1	1
b	1	1	1	1	1	3	3	1	1	1	1	3	1	1	1	1	3	1	1	1	1	1	1	3	1	1	1	1	3	1
c	1	1	1	1	1	1	3	3	1	1	1	1	3	1	1	1	1	3	1	1	1	1	1	1	3	1	1	1	1	3
d	1	1	1	1	1	1	1	3	3	1	1	1	1	3	1	1	1	1	3	1	3	1	1	1	1	3	1	1	1	1
e	1	1	1	1	1	1	1	1	3	3	1	1	1	1	3	1	1	1	1	3	1	3	1	1	1	1	3	1	1	1
f	3	1	1	1	1	1	1	1	1	3	3	1	1	1	1	3	1	1	1	1	1	1	3	1	1	1	1	3	1	1
g	3	3	1	1	1	1	1	1	1	1	1	3	1	1	1	1	3	1	1	1	1	1	1	3	1	1	1	1	3	1
h	1	3	3	1	1	1	1	1	1	1	1	1	3	1	1	1	1	3	1	1	1	1	1	1	3	1	1	1	1	3
i	1	1	3	3	1	1	1	1	1	1	1	1	1	3	1	1	1	1	3	1	3	1	1	1	1	3	1	1	1	1
j	1	1	1	3	3	1	1	1	1	1	1	1	1	1	3	1	1	1	1	3	1	3	1	1	1	1	3	1	1	1

of its nearest-neighbour vertices. If the frog has to make a minimum of h hops to get from vertex a to vertex b, then these two vertices are topologically hth neighbours to one another. (Of course, each vertex is a zeroth neighbour to itself). Both the columns and rows of the neighbourhood matrix are labelled alphabetically. Thus matrix element ab equals matrix element ba, and this element is the positive integer h.

Two finite lattices with neighbourhood matrices U and V are defined to be topologically identical if and only if there exists a permutation matrix P such that $UP = PV$. In particular, we are interested here in determining whether two geometrically distinct finite bipartite bcc lattices are topologically identical or distinct. If the initial vertex is at the origin, then the eight nearest neighbours would have coordinates $(\pm 1, \pm 1, \pm 1)$. The 26 topologically second neighbours to the origin would have coordinates of one of the three types $(2, 0, 0)$, $(2, 2, 0)$ or $(2, 2, 2)$, and the 56 topologically third neighbours would have coordinates of the types $(3, 1, 1)$, $(3, 3, 1)$, or $(3, 3, 3)$. None of our finite bcc lattices of $N < 32$ has any pair of topologically fourth neighbour vertices. Thus, for any bipartite finite bcc lattice of $N < 32$, every pair of vertices on the same sublattice are topologically second neighbours. One vertex on one sublattice and one on the other sublattice are topologically either nearest or third neighbours.

As an example, we consider the four geometrically distinct $N = 20$ bipartite bcc lattices. We label the vertices on one sublattice $A, B, \ldots, J$ and those on the other sublattice $a, b, \ldots, j$. The rows and the columns of the 20×20 neighbourhood matrices are labelled in the above order. Since every off-diagonal element in the upper-left quadrant and the lower-right quadrant of the neighbourhood matrix of each of the four lattices is 2, it is sufficient to consider only the distinguishable lower-left (or upper-right) quadrants. Three of the submatrices are displayed in table 3.

A visual inspection of such small submatrices as in table 3 will reveal which pairs are equivalent and which are distinct. Notice that the middle matrix representing lattice 20.2 consists of 'quartets' of vertices. For example, vertices A and F on one sublattice have in common the same two third-neighbour vertices, a and f, on the other sublattice. Each of the vertices belongs to one and only one such quartet. The matrix on the right demonstrates the same quartet structure for lattice 20.3. Obviously these two lattices are equivalent under

permutation, and so the two lattices they represent are topologically identical. However, the matrix on the left shows that any two vertices on one sublattice of lattice 20.1 have one and only one third neighbour in common on the other sublattice. Finite lattice 20.1 is topologically distinct from lattices 20.2 and 20.3. The computed ground-state properties of the Heisenberg antiferromagnet, i.e. the energy, staggered magnetization, and spin–spin correlations, each of them having different values on lattice 20.1 from the identical values on lattices 20.2, 20.3, and 20.4, confirm the topological classification derived by inspecting the neighbourhood matrices. (Lattice 20.4 is defined by the vectors $\boldsymbol{l}_1 = (2, 0, 4)$, $\boldsymbol{l}_2 = (0, 4, 0)$ and $\boldsymbol{l}_3 = (0, 0, 10)$.)

However, for larger N, simple inspection of the neighbourhood matrices is inadequate to sort the finite bipartite lattices topologically. Thus we define a nine-digit *sorting code* based on the lower-left quadrant of each neighbourhood matrix. For each finite lattice choose one of the sublattices and one the $N/2$ vertices on it, say A. Each vertex on the chosen sublattice, A included, will have zero to eight nearest neighbours on the other sublattice that are also nearest neighbours to A. The v_i vertices on the chosen sublattice will have i nearest neighbours in common with A. The topological sorting code is defined as

$$C \text{ (index)} = v_0, v_1, \ldots, v_8. \tag{3.1}$$

In table 3 it is easy to see for lattice 20.1 that vertices B and J have seven nearest neighbours in common with A and the other seven vertices on the same sublattice have six nearest neighbours in common with A. (Of course, A has eight nearest neighbours in common with A.) Thus the topological sorting code $C(20.1) = 000\,000\,721$. In lattices 20.2, 20.3 and 20.4 vertices F and A have eight nearest neighbours in common and each of the other eight vertices on this sublattice have six nearest neighbours in common with A; hence code $C(20.2) = 000\,000\,802 = C(20.3) = C(20.4)$. Thus these three lattices are topologically identical, according to the code. We have confirmed this identity, and several other identities, via computed values of the energy, staggered-magnetization and spin–spin correlations of the Heisenberg antiferromagnet. In some cases further confirmation of topological identity or distinction has been reinforced by the energy, magnetization and spin–spin correlations of the $S = \frac{1}{2}XY$ ferromagnet.

We have used another criterion for the topological classification of finite lattices, the Smith normal form [12]. For any square matrix, A, or finite rank, n, there exists just one matrix, F, also of rank n, in Smith normal form.

$$F = \begin{pmatrix} D & 0 \\ 0 & 0 \end{pmatrix} \tag{3.2}$$

where D is a diagonal matrix of rank $r \leqslant n$. The elements on the diagonal,

$$d_1 = b_1 = 1, \; d_2 = b_1 b_2, \ldots, \; d_r = b_1 b_2, \ldots, b_r. \tag{3.3}$$

The neighbourhood matrices of interest here are in the field of positive integers so b_i is integral. All equivalent matrices have the same Smith normal form, but the Smith matrix is unique to that one set of equivalent matrices.

The definition of the b_i is complicated and so is omitted here. However, the definition of b_i, the process of calculating a Smith normal form matrix and the proof of the above properties of the Smith normal form can be found in several texts on matrices, e.g. Turnbull and Aitken [13]. Hand calculation of the Smith normal form of a matrix of only integer elements and a rank as low as eight would be extremely tedious. However, programs to compute the Smith normal form for much larger matrices are readily available. We have used the Maple program.

As an example, here are the diagonal elements of the Smith normal forms for the lower-left quadrant of the neighbourhood matrices of the four $N = 20$ bipartite bcc lattices:

$$F(20.1) = 1, 2, 2, 2, 2, 2, 2, 2, 14, 0$$

and

$$F(20.2) = F(20.3) = F(20.4) = 1, 2, 2, 2, 14, 0, 0, 0, 0, 0.$$

It turns out that neither of the two methods, *by themselves*, are completely successful in finding all of the topologically identical sets of lattices. However, combining the two methods appears to find all of these sets. This was confirmed by examining the computed properties of the $S = \frac{1}{2}$ Heisenberg antiferromagnet on bipartite bcc lattices of $N \leqslant 30$. Thus we were able to greatly reduce the computer time to diagonalize this model on $N = 32$ lattices by using only one lattice of each topology as indicated by our sorting codes and Smith normal forms.

4. Computation of the ground sate properties of the $S = 1/2$ Heisenberg antiferromagnet on finite bcc lattices and statistical estimates of the zero temperature properties of this model on the infinite bcc lattice

The Hamiltonian of the spin one-half Heisenberg antiferromagnet in zero field is

$$H = -J \sum_{\langle i,j \rangle} \boldsymbol{S}_i \cdot \boldsymbol{S}_j \tag{4.1}$$

where the sum is over nearest-neighbour pairs of vertices. It was proved by Lieb and Mattis [14] that the ground state of this model on a bipartite three-dimensional lattice has total spin equal to zero and is nondegenerate. Later is was proved by Kennedy *et al* [15] and Kubo and Kishi [16] that this model has long-range Néel order in the ground state.

All our finite lattices and thus the corresponding Hamiltonians are translationally invariant as well as invariant under inversion, which simplifies the diagonalization of the Hamiltonians.

The diagonalization of the Hamiltonian matrix to obtain the ground-state eigenvalue (the energy) and the ground-state eigenvector has been done mostly by workstations and a Power Challenge computer at the University of Magdeburg with some input from Dalhousie's SP2 computer. The Lanczos technique used in the diagonalization is standard [17]. In order to diagonalize the Hamiltonian on the larger lattices we had to reduce the dimensions of the Hilbert space by using the translation and point group symmetries of the Hamiltonian. The largest Hamiltonian we diagonalized, on an $N = 32$ lattice, is of rank 4.7 million, approximately. Due to the limited precision of the computer, the precision of the ground-state eigenvalue (or energy) of the Hamiltonian on the larger lattices is seven or eight digits.

Using the ground-state eigenvector we have computed the ground-state spin–spin correlations, $\langle \boldsymbol{S}_i \cdot \boldsymbol{S}_j \rangle$, for all pairs of spins on all geometrically distinct bipartite bcc lattices of N vertices where $16 \leqslant N \leqslant 30$, and for $N = 32$ we have computed the energies and correlations of all *topologically* distinct bipartite lattices only.

The principal results are displayed in table 4 for all topologically distinct bipartite bcc lattices of $16 \leqslant N \leqslant 32$. For each lattice only the average correlations are displayed for topologically first-, second- and third-neighbour correlations. We have omitted fourth-neighbour correlations from table 4 because only some bcc lattices of $N \geqslant 32$ have fourth-neighbour pairs of vertices. The average of first-neighbour correlations is simply the ground-state energy per vertex divided by $4J$.

Table 4. The data below include the staggered magnetization per vertex, m^+, and first, second and third topological neighbour spin–spin correlations, Γ_1, Γ_2 and Γ_3, and the statistical weight, w_1, of Γ_1 (or the ground-state energy), of the $S = \frac{1}{2}$ Heisenberg antiferromagnet on all topologically distinct finite bcc lattices of $16 \leqslant N \leqslant 32$.

$N\alpha$	m^+	Γ_1	w_1	Γ_2	Γ_3
16*A*	0.559 0170	−0.312 500	0.996	0.250 000	—
18*A*	0.549 6565	−0.309 415	0.999	0.246 137	−0.243 779
20*A*	0.541 8660	−0.306 983	0.998	0.242 910	−0.240 163
20*B*	0.541 9474	−0.306 949	0.991	0.243 008	−0.240 741
22*A*	0.535 3653	−0.304 979	0.994	0.240 278	−0.237 650
24*A*	0.529 5492	−0.303 416	0.998	0.237 729	−0.234 435
24*B*	0.529 8510	−0.303 301	0.986	0.238 082	−0.235 625
24*C*	0.529 3639	−0.303 490	0.981	0.237 520	−0.237 700
24*D*	0.529 9500	−0.303 263	0.971	0.238 197	−0.236 017
24*E*	0.529 9674	−0.303 259	0.969	0.238 217	−0.236 080
24*F*	0.528 5647	−0.303 799	0.706	0.236 597	−0.230 544
26*A*	0.525 1659	−0.301 860	0.964	0.236 282	−0.234 103
26*B*	0.524 2474	−0.302 191	0.931	0.235 239	−0.231 066
28*A*	0.520 7211	−0.300 755	0.993	0.234 316	−0.231 678
28*B*	0.520 0785	−0.300 975	0.952	0.233 596	−0.229 824
28*C*	0.521 1685	−0.300 593	0.910	0.234 819	−0.232 982
28*D*	0.521 2568	−0.300 577	0.879	0.234 179	−0.233 244
28*E*	0.519 3081	−0.301 240	0.688	0.232 733	−0.227 603
28*F*	0.518 9486	−0.301 366	0.508	0.232 332	−0.226 563
30*A*	0.516 8641	−0.299 770	0.999	0.232 659	−0.229 789
30*B*	0.516 9294	−0.299 758	0.998	0.232 731	−0.230 024
30*C*	0.516 9302	−0.299 758	0.997	0.232 732	−0.230 028
30*D*	0.516 3136	−0.299 952	0.954	0.232 050	−0.228 439
30*E*	0.517 3857	−0.299 593	0.925	0.233 237	−0.231 225
30*F*	0.517 7871	−0.299 441	0.779	0.233 683	−0.232 289
30*G*	0.514 6583	−0.300 501	0.281	0.230 221	−0.224 155
32*A*	0.513 6234	−0.298 855	1.000	0.231 396	−0.228 763
32*B*	0.513 4834	−0.298 917	0.999	0.231 243	−0.228 414
32*C*	0.513 4433	−0.298 928	0.999	0.232 340	−0.228 320
32*D*	0.513 4277	−0.298 930	0.995	0.232 325	−0.228 286
32*E*	0.513 7568	−0.298 812	0.982	0.231 542	−0.229 141
32*F*	0.513 8191	−0.298 780	0.969	0.231 611	−0.229 962
32*G*	0.514 1207	−0.298 684	0.920	0.231 941	−0.229 957
32*H*	0.514 1236	−0.298 684	0.908	0.231 945	−0.229 962
32*I*	0.512 8576	−0.299 116	0.908	0.231 739	−0.226 930
32*J*	0.514 3656	−0.298 600	0.829	0.232 778	−0.226 091
32*K*	0.514 5824	−0.298 521	0.786	0.231 709	−0.229 962
32*L*	0.512 5163	−0.299 255	0.737	0.230 104	−0.219 460
32*M*	0.511 6581	−0.299 480	0.478	0.229 246	−0.224 108
32*N*	0.511 5721	−0.299 515	0.426	0.230 421	−0.223 898
32*P*	0.510 2774	−0.299 915	0.002	0.229 101	−0.210 851
32*Q*	0.509 6882	−0.300 104	0.000	0.233 290	−0.230 544

A prime example of the importance of topology rather than geometry is found in $N = 32$ bipartite bcc lattice $32J$. Each vertex has eight first neighbours, 14 topologically second neighbours, eight topologically third neighbours and one topologically fourth neighbour. For all 14 second neighbour pairs, $\langle \boldsymbol{S}_0 \cdot \boldsymbol{S}_i \rangle = 0.233\,290$, although *geometrically* only six of these 14 neighbours are second neighbours, six are third neighbours and two neighbours are fifth neighbours to the vertex chosen as origin. All topologically third-neighbour pairs are geometrically fourth-neighbour pairs and all have the same spin–spin correlation. Similarly all first-neighbour pairs have the same correlation, as in table 4. As a geometric entity this lattice has rotationally complete cubic or octahedral symmetry, O_h. However, as a topological entity lattice $32J$ has a still *greater* symmetry demonstrated by the second neighbour correlations.

To obtain estimates of a physical property of the $S = \frac{1}{2}$ Heisenberg antiferromagnet on the infinite bcc lattice at zero temperature we first fit a formula in inverse powers of L ($L^3 = N$) to the ground-state data for that property on each of the topologically distinct finite bcc lattices of $N \leqslant 32$ vertices. For instance, spin-wave theory [1] and other studies [18–20] show that the dimensionless ground-state energy per vertex, $\varepsilon_0 = E_0/NJ$, fits the formula

$$\varepsilon_0(L) = \varepsilon_0(\infty) + A_4 L^{-4} + A_6 L^{-6} + \cdots. \tag{4.2}$$

Because ε_0 is simply four times the average of the nearest-neighbour correlations, we use the same formula to fit the topologically second- and third-neighbour correlations.

The dimensionless staggered magnetization operator,

$$\boldsymbol{M}^+ \equiv \sum_{i=1}^{N/2} \boldsymbol{S}_i - \sum_{j=1}^{N/2} \boldsymbol{S}_j \tag{4.3}$$

where the $\boldsymbol{S}_i$ are on one sublattice and the $\boldsymbol{S}_j$ on the other. In the absence of an external field $\langle \boldsymbol{M}^+ \rangle = 0$, but

$$\langle (\boldsymbol{M}^+)^2 \rangle / N = \sum_{k=1}^{N} |\langle \boldsymbol{S}_i \cdot \boldsymbol{S}_j \rangle| \tag{4.4}$$

is nonzero. The staggered magnetization per vertex, m^+, is calculated using

$$m^+ = [\langle (\boldsymbol{M}^+)^2 \rangle]^{1/2}/N. \tag{4.5}$$

Spin-wave theory [1] shows only that

$$m^+(L) = m^+(\infty) + B_2 L^{-2} + \cdots. \tag{4.6}$$

After some testing of various powers of L in a statistical analysis of the data, we have settled on using as a third term $B_4 L^{-4}$; we have also tested a two-parameter fit.

Our fitting was done using the statistical programming package S-PLUS (produced by MathSoft Inc., Seattle, USA). We have also obtained valuable advice from Wade Blanchard, an expert statistical analyst in Dalhousie's Department of Mathematics and Statistics. First we perform for each property a standard least-squares fit of the data from all the topologically distinct lattices to the appropriate formula. Then each data point is assigned a weight, $\sin(u)/u$, determined by the Huber weight function [21]. The weights range from 1 for a point directly on the best fitted curve to 0 for a distant outrider. Weights for the energies are shown in table 4.

Blanchard advised us that cut-off weights are usually about 0.80, although this cut-off depends on the data being used. We have varied the energy cut-off weights, w_c, from as high as 0.95, which would classify 19 of the 42 distinct lattices as outriders, to as low as

Table 5. Estimates (with confidence limits) of the $T = 0$ properties of the $S = \frac{1}{2}$ Heisenberg antiferromagnet on the infinite bcc lattice.

Method	$-\varepsilon_0$	$-A_4$	A_6	m^+	B_2	B_4	Γ_2	$-\Gamma_3$
finite lattice	1.1518(9)	5.24(10)	8.2(6)	0.4409(11)	0.70(1)	0.30(7)	0.2161(6)	0.214(3)
spin wave [1]	1.1512(1)	4.5	—	0.4412(3)	0.72	—	—	—
series [1]	1.1510(5)	—	—	0.442(4)	—	—	—	—
variation	1.160	—	—	0.426	—	—	—	—

0.75, which would classify only nine of the lattices as outriders. The estimates of both the energy and staggered magnetization peak as a function of w_c when $w_c = 0.85$ or, alternatively, where the number of outriders, N_0, is 12. Although the energy and staggered magnetization weights are similar, we decided to use the energy weights to define outriders because the energy is simply the ground-state eigenvalue of the Hamiltonian matrix, where the staggered magnetization is calculated from the ground-state eigenvector. Thus for each N we were able to rank those bcc lattices that were not outriders with bcc lattice *NA* being 'best', lattice *NB* second best, etc, as seen in table 2. The confidence limits that we have inserted in table 5 after the estimates of most properties are determined as the difference between the estimates for $N_0 = 12$ and the estimates for $N_0 = 11$ and $N_0 = 13$.

Table 5 displays our finite-lattice method estimates at zero temperature of the physical properties of the spin one-half Heisenberg antiferromagnet on the infinite bcc lattice together with estimates by three other methods. According to the variational estimate of the energy per vertex, ε_0, the other three estimates are too high by at least 1%, although they agree with one another to within 0.05%. The finite-lattice estimate of the staggered magnetization per vertex, m^+, agrees with the third-order spin-wave and series-expansion estimates to within 0.25%. Some readers may notice that the spin-wave estimates of A_4 and B_2 displayed in this table are different from those in [1]. The reason is that the authors in that article define L as $L^3 = N/2$.

The statistical analysis of the second- and third-neighbour correlations on the infinite lattice have been made not only directly but also by analysis of the ratios of, and differences between, the first-, second- and third-neighbour correlations. The resulting variation among the estimates of Γ_2 and Γ_3 led to our confidence limits. To the best of our knowledge, no other estimates of these correlations have been published.

Following the example of Oitmaa *et al* [1] we can use our estimates in table 5 to calculate other properties. The spin-wave velocity $v = -A_4/\beta$ where, using our definition of L and the geometric quantity of Hasenfratz and Leutwyler [20], $\beta = 2.110\,4607$ so our estimate is $v = 2.48(15)$. Another geometric property of the bcc lattice [19] is $\gamma = 0.179\,205\,77$. Then our estimate of the spin stiffness, $\rho_s = m^+(\infty)v\gamma/B_2 = 0.280(11)$. Finally, the perpendicular susceptibility $\chi_\perp = \rho_s/v^2 = 0.046(2)$. The most direct estimate among the above three, for us and for Oitmaa *et al* [1], is that of the spin-wave velocity, v. The third-order spin-wave estimate 2.2 is as good as we might expect in view of the large confidence limits in each case.

5. Summary, conclusions and outlook

Following the example of earlier definitions, first of finite simple cubic lattices [8] and second of fcc lattices [9], we have in this paper defined finite bipartite bcc lattices. In each step improvements have been made, first in introducing finite lattices in three dimensions, next on introducing the defining vectors in the upper triangular lattice form and now in classifying bipartite finite lattices *topologically*, an important step beyond geometric classification. Indeed to establish our topological classification we have introduced an entity, the *topological neighbourhood matrix*.

Geometrically distinct but topologically identical finite lattices have neighbourhood matrices that look superficially distinct but are mathematically identical. Because for finite lattices with a small number of vertices the neighbourhood matrices are very simple, we have been able to derive from them a simple topological code to sort out finite bipartite bcc lattices, a type of sorting code that would work equally well on simple cubic or other lattices.

We have also used the old but largely unfamiliar Smith normal form of the neighbourhood matrix as an alternate way to sort finite lattices topologically. The Smith matrix is much more complicated to derive from the neighbourhood matrix than is our sorting code, but it would work for quite large lattices well beyond the scope of our simpler method. When both methods answered that two lattices were topologically distinct, the ground-state properties of the Heisenberg Hamiltonian on these two lattices invariably confirmed this fact.

We have diagonalized the spin one-half Heisenberg antiferromagnet Hamiltonian on all geometrically distinct bipartite bcc lattices of sixteen to twenty vertices. Using both our methods of recognizing topologically identical bipartite lattices, we have diagonalized the Hamiltonian on only sixteen topologically distinct thirty-two vertex bipartite bcc lattices, thus saving many hours of computing time. The high-performance computer used standard procedures to compute to very high precision the ground-state eigenvalue (energy) and eigenvector on each lattice. Thence all spin–spin correlations and the staggered magnetization were derived, and other properties such as four-spin correlations could have been derived.

These data for each physical property were fitted statistically to appropriate equations using inverse powers of L, the cube root of the number of vertices. Unlike some methods, our finite-lattice method enables the determination (statistically) of the confidence limits of the estimates of each property calculated.

We were pleased to find that our estimate of the energy per vertex of the Heisenberg antiferromagnet on the infinite bcc lattice at zero temperature agrees with the third-order spin-wave and series-expansion estimates of Oitmaa *et al* [1] to within five parts in ten thousand. Our estimate of the staggered magnetization agrees with the spin-wave estimate [1] to within 0.25% and within the 1% confidence limits of the series estimate. Variational estimates of energy and staggered magnetization [11] differ from those of the other three methods by a larger amount. We have not found calculations by other methods of the second- and third-neighbour spin–spin correlations that we have calculated, but our estimates are useful because the correlations give insight into the nature of the ground-state eigenvector.

We would like to see by other theoretical methods, such as the quantum Monte Carlo method, estimates of the properties we have calculated. Also we failed to find in the literature experimental measurements of energy and staggered magnetization at near zero temperature on magnetic materials that can be well represented by the spin one-half Heisenberg antiferromagnet on the bcc lattice.

A nearly ideal three-dimensional isotropic Heisenberg antiferromagnet is the magnetic system of $RbMnF_3$ [22], but the magnetic moments have $5/2$ spins. Experimental examples of a spin one-half isotropic Heisenberg antiferromagnet on a bcc lattice have been hard to find, but very recently Srdanov *et al* [23] have found evidence for a spin one-half Heisenberg bcc antiferromagnet consisting of F centres in sodium-electro-sodalite.

Perhaps the greatest advance described in this paper is the recognition of the importance of topology in the theoretical study of quantum spin systems at zero temperature. We have learned a lot in the past two or three years, but there is much more to learn and do in this corner of physics—studying other lattices, different properties, higher spin, nonzero temperature, etc. More powerful computers would help us, and they will become available. Better still, we invite theoretical and experimental colleagues to join us in our exploration.

Acknowledgments

We are grateful to colleagues H Nishimori, P Keast, W Blanchard and W Zheng for their useful advice. Part of this paper was written when DDB was a Visiting Professor at the University of New South Wales. This research has been supported in part by the Natural Sciences and Engineering Research Council of Canada and by Deutsche Forschungsgemeinschaft (project Ri 615/1-2).

References

[1] Oitmaa J, Hamer C J and Zheng W 1994 *Phys. Rev.* B **50** 3877
[2] Bonner J and Fisher M E 1964 *Phys. Rev.* **153** A640
[3] Betts D D and Oitmaa J 1977 *Phys. Lett.* **62A** 277
[4] Oitmaa J and Betts D D 1978 *Can. J. Phys.* **56** 897
[5] Manousakis E 1991 *Rev. Mod. Phys.* **63** 1
[6] Dagatto E 1994 *Rev. Mod. Phys.* **66** 763
[7] Oitmaa J and Betts D D 1978 *Phys. Lett.* **68A** 450
[8] Betts D D and Stewart G E 1977 *Can. J. Phys.* **75** 47
[9] Stewart G E, Betts D D and Flynn J S 1997 *J. Phys. Soc. Japan* **66** 3231
[10] Lyness J N, Sorevik T and Keast P 1991 *Math. Comput.* **56** 243
[11] Olés A M and Olés B 1993 *J. Phys.: Condens. Matter* **5** 8403
[12] Smith H J S 1861 *Phil. Trans. R. Soc.* **151** 293
[13] Turnbull H W and Aitken A C 1932 *An Introduction to the Theory of Canonical Matrices* (Glasgow: Blackie) pp 21–3
[14] Lieb E H and Mattis D C 1962 *J. Math. Phys.* **3** 749
[15] Kennedy T, Lieb E H and Shastry B S 1988 *J. Stat. Phys.* **53** 1019
[16] Kubo K and Kishi T 1988 *Phys. Rev. Lett.* **61** 2585
[17] Cullum J K and Willoughby R A 1985 *Lanczos Algorithms for Large Symmetric Eigenvalue Computations* (Boston, MA: Birkhhauser)
[18] Neuberger H and Ziman T 1989 *Phys. Rev.* B **39** 2608
[19] Fisher D S 1989 *Phys. Rev.* B **39** 11783
[20] Hasenfratz P and Leutwyler H 1990 *Nucl. Phys.* B **343** 241
[21] Hoaglin D C, Mostelle F and Tukey J W 1983 *Understanding Robust and Exploratory Data Analysis* (New York: Wiley) p 366
[22] Coldea R, Cowley R, Ferring T G, McMorrow D F and Roessli B 1998 *Phys. Rev.* B **57** 5281
[23] Srdanov V I, Stucky G D, Lippmaa E and Engelhardt G 1998 *Phys. Rev. Lett.* **80** 2449